Spectral-domain modelling of Wave Energy Converters as an efficient tool for adjustment of PTO model parameters

Jian Tan and Antonio Jarquin Laguna

Abstract—**The power take-off (PTO) system is a core component in wave energy converters (WECs) as it plays a critical role in power production. In numerical models the PTO systems are commonly represented and simplified through a combination of linear stiffness and damping terms in the equations of motion. These parameters are influential to the dynamic response and thus affect the power performance of WECs. In the preliminary design and optimization of WECs, proper tuning of the PTO damping and stiffness could reflect better the potential of the concept. In practice, the PTO damping and stiffness are tuned to maximize the absorbed power by achieving the desired velocity amplitude or phase of the velocity with respect to the excitation force. However, recent literature has indicated that the selection of PTO parameters for maximum mechanical power absorption is not necessarily optimal for the maximum production of electrical power when the conversion efficiency of the electrical machine is included. To obtain these parameters which maximize the delivered electrical power, wave-to-wire models are widely used. Nevertheless, wave-to-wire models are predominately established by using time-domain models which can be associated with large computational efforts from the perspective of early-stage design and concept evaluation. To tackle this challenge, a spectral-domain-based wave-to-wire model is proposed to cover both hydrodynamic and electrical responses. In this paper, a spherical heaving point absorber integrated with a linear permanent-magnet generator is used as a reference. The relevant nonlinear effects are incorporated by statistical linearization using spectral-domain modelling. In particular, the nonlinear effects considered in this work include the viscous drag force, the electrical current saturation and the partial overlap between the translator and stator components of the linear generator. The model results are then verified against a nonlinear time-domain-based wave-to-wire model. Subsequently, the proposed model is applied to identify the PTO parameters for maximizing the electrical power in various wave states. The computational efficiency and accuracy of the proposed spectral-domain model are compared with the time-domain model, with regard to the identification of the proper PTO damping coefficients. Based on the results, the advantage of using the spectral-domain-based wave-to-wire modeling in PTO tuning is demonstrated.**

Index Terms—**Wave energy converter, spectral domain modeling, wave-to-wire modeling, PTO parameters**

I. Introduction

AS a kind of untapped energy resource, ocean waves carry a tremendous amount of renewable energy. However, the technology of wave energy converters (WECs) still has a distance to large-scale commercialization. To improve the competitiveness of existing WECs, it is of essence to further iterate the design and technology. Given the high efficiency and low expense, numerical models are widely applied to take the job. Hence, numerical models play an important role in accelerating the development of WECs.

Wave-to-wire (W2W) modeling is a numerical method used to evaluate the performance of wave energy converters (WECs) [1]. This modeling technique provides a comprehensive analysis of the complete operation process, including wave-buoy hydrodynamics, energy transmission, and electricity generation [2]. As a result, W2W models enable systematic analysis of the performance of WECs. Numerous W2W models have been proposed and validated in recent years [3]–[5]. These models offer a more complete picture of WEC devices than pure hydrodynamic models. Power Take-Off (PTO) parameters are often tuned based on hydrodynamic models to maximize the absorbed mechanical power by achieving the desired floater velocity or phase [6], [7]. However, recent studies have shown that the conversion efficiency of electrical generators strongly depends on the PTO parameters [8], [9]. PTO parameters that optimize the absorption of mechanical power may not necessarily optimize the production of electrical power. This is a limitation of hydrodynamic models alone, which cannot capture this effect. Furthermore, the conversion efficiency of electrical generators in PTO systems is strongly influenced by the operating conditions of WECs [10], [11]. For example, the efficiency of a linear generator applied in a point absorber can vary from around 70 % in high-frequency waves to 20 % in low-frequency waves. Neglecting the modeling of the electrical generators can result in poor estimates of the PTO parameter of WECs. Therefore, relying solely on hydrodynamic models for the design and optimization of WECs is insufficient. Developing W2W models that incorporate the electrical generator is crucial for a more comprehensive analysis. Existing W2W models are primarily based on the time-domain (TD) approach to capture nonlinear effects in power absorption, transmission, and conversion stages. However, since WEC technology is still in a premature phase, the design and optimization require numerous iterations. Using TD W2W models can signifi-

J. Tan and A. J. Laguna are with the Department of Maritime & Transport Technology, Delft University of Technology, The Netherlands (e-mail: A.JarquinLaguna@tudelft.nl)

Digital Object Identifier:
https://doi.org/10.36688/ewtec-2023-278.

cantly increase the computational time required. Thus, developing computationally-efficient W2W models is essential for concept and design exploration and in general for advancing WEC technology toward large-scale commercialization.

Spectral-Domain (SD) modeling has emerged as a promising numerical technique in the field of WECs due to its high computational efficiency. Recent investigations [12], [13] have shown that SD modeling can be thousands of times faster than TD modeling, with a relative error of no more than 5 % in operational regions. In principle, SD modeling is formulated based on the framework of Freqeuncy-Domain (FD) modeling. However, unlike conventional FD modeling, SD modeling incorporates nonlinear effects through stochastic linearization, which assumes that the system's response can be represented by a Gaussian distribution. One of the first applications of SD modeling to WECs was reported in [12], where a flap-type WEC was modeled with quadratic damping and wave force decoupling due to large amplitude motions. The results from SD modeling were found to agree well with TD modeling. Since then, SD modeling has been further developed to include various effects such as end-stop force, mooring force, viscous drag force, Coulomb damping, nonlinear hydrostatic force, and PTO force constraint [13]–[18]. However, while SD modeling has been shown to accurately predict hydrodynamic responses, its applicability to integrating electrical modeling is still unclear. As W2W models must reflect the behavior of electrical components, in combination with hydrodynamic responses, there is a need for further research to extend SD modeling to cover the complete W2W process.

The objective of this study is to develop a numerical model, specifically a SD W2W model, to adjust the PTO parameters. The model incorporates a heaving spherical point absorber that is connected to a linear permanent magnet generator and a power converter. By utilizing this model, it becomes possible to predict the statistical responses of both the power absorption and power conversion stages of WECs. The model takes into account factors such as PTO force saturation, viscous drag force, the partial overlap between the translator and stator of the linear generator, and the stator current limit. In order to validate the model, the results obtained from the proposed SD W2W model are compared with those obtained from a nonlinear TD W2W model. Furthermore, the performance of the proposed SD W2W model in the adjustment of PTO parameters is demonstrated for various wave conditions.

II. Concept description

While it is feasible to develop SD W2W models for different configurations of captors and PTO systems, the scope of this research is centred on a specific configuration. Specifically, it focuses on the combination of a heaving point absorber concept with a linear PM generator. This particular configuration has garnered considerable attention in recent years and has been extensively studied in terms of both its hydrodynamic and electrical properties. Previous works such as [19]–[21] have effectively demonstrated the characteristics of this single degree-of-freedom concept. Therefore, it serves as a suitable and representative reference for validating the proposed model.

In Figure 1, a schematic representation of the investigated WEC (Wave Energy Converter) concept is presented. The WEC consists of a floating buoy connected to a PTO (Power Take-Off) system that is anchored to the ocean floor. The floating buoy is characterized by a spherical shape with a diameter of 5 m. It is designed to partially submerge in calm water, meaning that its density is equal to half that of water. When stimulated by incoming ocean waves, the buoy undergoes vertical oscillations, resulting in the conversion of wave energy into mechanical power absorption.

In order to convert the absorbed mechanical power into usable electrical power, a linear PM (Permanent Magnet) generator is utilized as the PTO system in the WEC concept. The translator component of the generator is directly connected to the buoy through a rigid link. To balance the attractive forces, two identical machines are symmetrically placed within the generator. The electrical inverter, connected to the output side of the machine, is implemented as a three-phase back-to-back converter [20]. The design of this generator is inspired by the electrical machine used in the AWS (Aquabuoy Wave Energy System) wave energy converter [22]. However, it has been scaled down from the original reference machine to match the dimensions of the buoy employed in this study. The scaling process follows the principle of maintaining an identical force density per unit area of the active surface of the electrical machines. More detailed information regarding the scaling of electrical machines can be found in [11]. Since the translator length, force limit, and stator current limit of the generator have an impact on the nonlinearities addressed in this work, their parameters are adjusted in specific simulation cases to assess their influence on the accuracy of the proposed model. Unless otherwise specified, the machine parameters considered in this study are outlined in Table I.

III. Methodology

This section starts with presenting the conventional approach to derive the W2W model in the TD context. Next, the mathematical representation of the SD modeling is derived, and the stochastic linearization for incorporating the relevant nonlinear effects is introduced.

A. Time-domain approach

1) Representation of incoming waves: The incident waves are modeled using linear wave theory [23]. Based on the superposition, irregular waves are expressed as

$$\eta_{irr}(t) = \sum_{j=1}^{N} \zeta_a(\omega_j) \cos\left(k(\omega_j)x - \omega_j t + \varphi(\omega_j)\right) \qquad (1)$$

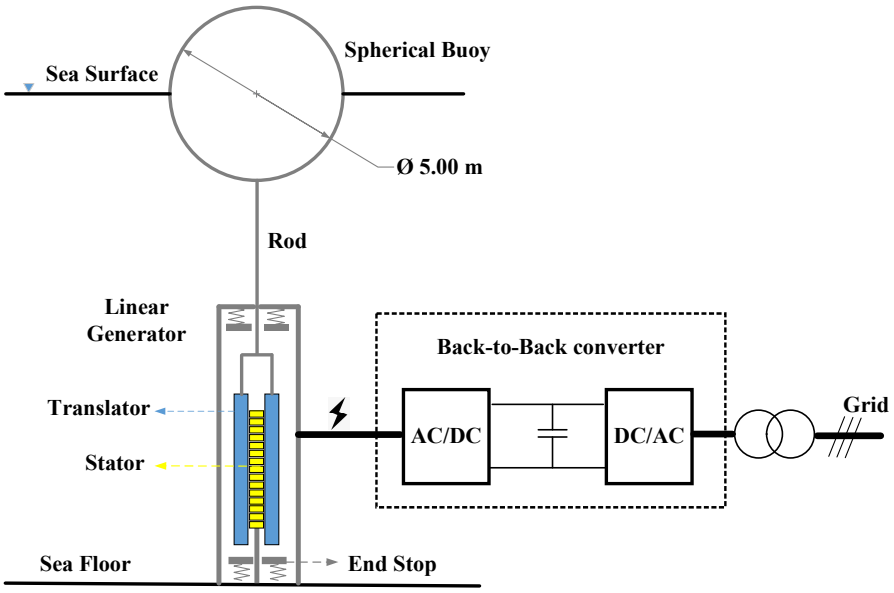

Fig. 1: Schematic of the spherical heaving point absorber with a bottom-founded linear PM generator [10].

TABLE I: Specification of the sized generator.

Parameters	Symbol	Quantities
Maximum average power	P_{rated}	220 kW
Maximum force	F_m	100 kN
Maximum velocity	u_{max}	2.2 m/s
Stroke	S	5.0 m
Translator length	L_{tra}	3.0 m
Stator length	L_{sta}	2.3 m
Stack length	l_s	0.46 m
Air gap length	g	5 mm
Slot width	b_s	15 m
Magnet pole width	b_p	79 mm
Tooth width	b_t	18.3 mm
Pole pitch	τ_p	100 mm
Slot pitch	τ_s	33.3 mm
Stator yoke height	h_{sy}	50 mm
Slot height	h_s	85 mm
Magnet thickness	l_m	15 mm
Recoil permeability of the magnets	μ_{rm}	1.1
Remanent flux density of the magnets	B_{rm}	1.1 T at 85 °C
Iron loss per unit mass	P_{Fe0}	4.9 W/kg at 50 Hz and 1.5 T
Copper resistivity	ρ_{Cu}	0.0252 $\mu\Omega$m at 120 °C
Copper fill factor	k_{sfil}	0.6
Number of conductors per slot	N_s	6
Number of slots per pole per phase	N_p	1

where t is the time; $k(\omega_j)$, $\zeta_a(\omega_j)$ and $\varphi_(\omega_j)$ are the wave number, wave amplitude and phase of the regular wave component corresponding to ω_j. Although the JONSWAP spectrum is applied in this work, the expression (1) is applicable for various types of wave spectrum [24].

2) Hydrodynamic modeling: The interaction between the floating buoy and the incoming waves is characterized using hydrodynamic modeling. The buoy is restricted to move solely in a heaving direction, and this degree of freedom is the focus of discussion. The motion of the floating buoy can be described in TD using the Cummins equation [25] as follows:

$$\big[M + M_r(\infty)\big]a(t) = F_e(t) + F_{pto}(t) + F_{hs}(t) + F_{vis}(t) + \int_{-\infty}^{t} K_{rad}(t-\tau)v(\tau)d\tau \tag{2}$$

in which M is the mass of the oscillating body, F_e is the excitation force, F_{hs} is the hydrostatic force, K_{rad} is the radiation impulse function, F_{pto} is the PTO force (or generator force); v and a are the velocity and acceleration of the buoy, and F_{vis} is the viscous drag force. $M_r(\infty)$ and K_{rad} represent the added mass evaluated at the infinite frequency and the radiation impulse function. They are calculated based on the

results of hydrodynamic damping $R_r(\omega)$ and added mass $M_r(\omega)$. To improve the computational efficiency, the convolution integral of the radiation force is approximated by a state-space representation [26].

According to [16], the viscous drag force can be estimated by a quadratic damping force, expressed as

$$F_{vis} = -\frac{1}{2}\rho C_D A_D |v(t)|v(t) \tag{3}$$

where ρ is the water density, C_D is the drag coefficient and A_D is the characteristic area of the buoy perpendicular to the moving direction. The values of the drag coefficient are selected based on the study presented in [27], in which the research geometry was the same as that in the present work.

In practice, the maximum force that the electrical generator can withstand is restricted by its designed capacity. Therefore, when the force approaches or exceeds this limit, the generator force becomes saturated. To incorporate the effect of force saturation, the generator force can be expressed as follows:

$$F_{pto}(t) = \begin{cases} -R_{pto}u(t), & \text{for} \quad |R_{pto}v(t)| \leq F_m \\ \text{sign}[-R_{pto}v(t)]F_m, & \text{for} \quad |R_{pto}v(t)| > F_m \end{cases} \tag{4}$$

where F_m embodies the PTO force limit.

3) Generator modeling: In this study, an analytical electrical model is utilized to evaluate the performance of the linear generator. The primary function of the linear generator is to convert the absorbed mechanical energy into usable electricity. The design parameters of the generator can be found in Table I. According to [20], the responses of the generator to the motion of the buoy can be described using an analytical model. As the buoy's movement causes relative motion between the translator and stator of the machine, it induces a no-load voltage. The root mean square value of the induced voltage over each pole pitch can be calculated as follows:

$$E_p(t) = \sqrt{2}N_m v(t) p l_s N_s k_w |\hat{B}_{gm}| K_{par}(t) \tag{5}$$

where $\hat{B}_{gm}$ is the fundamental space harmonic of the magnetic flux density in the air gap resulting from the magnets [20], p is the number of pole pairs, l_s is the stack length, N_s is the number of conductors per slot, and k_w is the winding factor. N_m is the machine number, which is set as 2 since the considered linear generator is double-sided. K_{par} is defined as the partial overlap factor, expressed as

$$K_{par} = \frac{l_{act}}{L_{sta}} \tag{6}$$

where l_{act} is the actual length of the overlap between the stator and translator, L_{sta} is the stator length. l_{act} is related to translator displacement, and it can be calculated as

$$l_{act}(z) = \begin{cases} L_{sta}, & |z| < 0.5(L_{tra} - L_{sta}) \\ 0, & |z| > 0.5(L_{tra} + L_{sta}) \\ 0.5(L_{tra} + L_{sta}) - |z|, & \text{else} \end{cases} \tag{7}$$

where z denotes the displacement of the buoy.

The partial overlap is a nonlinearity specific to linear generators. It arises due to the translator length typically being slightly longer than the stator length, as a compromise between cost and machine performance. This partial overlap has a detrimental effect on the efficiency of the generator. The reason is that a portion of the stator material does not experience the magnetic induction from the magnets mounted on the translator. As a result, the total induced no-load voltage decreases, requiring an increase in the stator current to supply the necessary generator force.

The iron losses are dependent on the generator frequency, which can be calculated as

$$P_{Fes} = P_{Fe0}\big[M_{Fest}\big(\frac{\hat{B}_{st}}{B_0}\big)^2 + M_{Fesy}\big(\frac{\hat{B}_{sy}}{B_0}\big)^2\big]\frac{f_e}{f_0}K_{par} \tag{8}$$

where P_{Fe0} is the iron loss per unit mass at the frequency f_0 and flux density B_0; M_{Fest} and M_{Fesy} are the mass of the stator teeth and the stator yoke respectively; f_e is the electrical generator frequency which is dependent on the buoy velocity, and $\hat{B}_{st}$ and $\hat{B}_{sy}$ embody the fundamental space harmonic of magnetic flux density in the stator teeth and yoke. $\hat{B}_{st}$ and $\hat{B}_{sy}$ can be calculated as

$$\hat{B}_{st} = \hat{B}_{gm}\frac{\tau_s}{b_t} \tag{9}$$

$$\hat{B}_{sy} = \hat{B}_{gm}\frac{\tau_p}{\pi h_{sy}} \tag{10}$$

where τ_s and τ_p are the slot pitch and pole pitch; b_t and h_{sy} are the tooth width and stator yoke height. The generator frequency is calculated as

$$f_e(t) = \frac{2\pi|v(t)|}{2\tau_p} \tag{11}$$

The power taken by the generator winding is expressed as the balance of absorbed mechanical power from iron losses, and it is expressed as

$$P_{wd} = F_{pto}(t)v(t) - P_{Fes} \tag{12}$$

During operation, the iron losses are negligible compared with the absorbed power [10]. Besides, in order to achieve higher system efficiency, the stator current I_s is regulated to be in phase with the no-load voltage E_p [20]. Therefore, (12) can be updated as

$$P_{wd} \approx F_{pto}(t)v(t) \tag{13}$$

From the perspective of electrical machines, the power taken by the winding is then transferred to electrical power, which can be expressed as

$$P_{wd} = mE_p(t)I_s(t) \tag{14}$$

where m represents the phase number of the electrical machine, and it is three in this case. It can be deduced from (13) and (14) that the linkage between the generator modeling and hydrodynamic modeling is built based on the balance between the power taken by the winding and the absorbed mechanical power. Substituting (5) to (13) and (14) gives the expression of the stator current:

$$I_s(t) = \frac{F_{pto}(t)}{m\sqrt{2}N_m p l_s N_s k_w |\hat{B}_{gm}| K_{par}(t)} \tag{15}$$

In electrical machines, there is an additional nonlinearity introduced by the electronic components, specifically the stator current limit I_{limit}. When the stator current approaches the limit, it reaches a saturation point and cannot increase further. The stator current limit is typically implemented to prevent the generator from overheating. It plays a significant role in determining the delivered grid power and overall system performance. Therefore, accounting for this effect is crucial in accurately evaluating the system's performance and ensuring its proper operation.

As observed from equation (15), the stator current is directly linked to the PTO force. Consequently, the saturation of the PTO force is intrinsically influenced by the current limit. The impact of the current limit is equivalent to that of the PTO force limit in hydrodynamic modeling. Hence, there is no need to separately incorporate the stator current constraint in the generator modeling. For a given electrical machine, the force limit F_m is correlated with the stator current limit I_{limit} in the following manner:

$$F_m = m\sqrt{2}N_m p l_s N_s k_w |\hat{B}_{gm}| I_{limit} \tag{16}$$

After the current I_s is derived, the copper losses can be calculated as

$$P_{copper}(t) = mI_s^2(t)R_t \tag{17}$$

where R_t is the stator phase resistance. For simplification, the converter losses P_{conv} are assumed to be only related to the generator side in this model, which can be expressed as

$$P_{conv} = \frac{P_{convm}}{31}\left[1 + 20\frac{|I_s(t)|}{I_{sm}} + 10\left(\frac{I_s(t)}{I_{sm}}\right)^2\right] \tag{18}$$

where P_{convm} is the power dissipation in the converter at the rated operating point, and it is assumed to be 3 % of the converter's rated power [28]; I_{sm} is rated current of the converter. In (18), the first term is a small constant part standing for the power dissipated in power supplies, gate drivers, control, and cooling system; the second term accounts for the major part that is proportional to the current, and this part is mainly related to the switching losses and conduction losses; the third term is proportional to the current squared, which corresponds to the conduction losses [28].

As the electrical losses have been derived, the electrical power delivered to the grid can be expressed as

$$P_{grid}(t) = P_{wd}(t) - P_{copper}(t) - P_{Fes}(t) - P_{conv}(t) \tag{19}$$

B. Spectral-domain approach

SD models are developed within the framework of FD modeling. In SD modeling, nonlinear effects are represented by equivalent linear coefficients in the equations of motion. These equivalent linear coefficients are determined through the process of stochastic linearization. Previous studies in the literature have primarily focused on using SD models to predict the hydrodynamic responses of WECs [12], [14], [16], [29]. However, in this subsection, the SD modeling approach is extended to encompass the responses of electrical machines as well. The typical nonlinear effects arising from the electrical generator are linearized and incorporated into the SD model. By integrating these developments, the derived model allows for the calculation of the entire wave-to-wire responses using a purely SD approach. Figure 2 provides a visual representation of the structure and solution process of the proposed SD W2W model.

1) Hydrodynamic modeling: It is assumed that the response of the system can be represented by a set of frequency components with random phases. Then, according to Newton's second law, the motion of the WEC as a rigid body in FD can be described as

$$\hat{F}_e(\omega) = [R_r(\omega) + R_{pto,eq} + R_{vis,eq}]\hat{v}(\omega) + \mathrm{i}\omega\hat{v}(\omega)[M + M_r(\omega)] + \mathrm{i}\hat{v}(\omega)(-\frac{K_{hs}}{\omega}) \tag{20}$$

where $R_r(\omega)$ is the hydrodynamic damping coefficient, R_{pto} is the PTO damping coefficient, ω is the angular wave frequency, $M_r(\omega)$ is the added mass of the buoy, $\hat{v}$ is complex amplitude of the vertical velocity, K_{hs} is the hydrostatic stiffness, and $R_{pto,eq}$ and $R_{vis,eq}$ represent the equivalent linear coefficients for the PTO force saturation and viscous force. Then, by solving (20), the complex amplitude of velocity $\hat{u}$ could be obtained as

$$\hat{v}(\omega) = \frac{\hat{F}_e(\omega)}{R_r(\omega) + +R_{pto,eq} + R_{vis,eq} + \mathrm{i}\omega[M + M_r(\omega)] - \mathrm{i}\frac{K_{hs}}{\omega}} \tag{21}$$

In a predefined wave spectrum, the amplitude of the wave component is related to the wave energy spectrum S_{ζ_a}, as

$$\zeta_a(\omega_j) = \sqrt{2S_{\zeta_a}(\omega_j)\Delta\omega} \tag{22}$$

The variance of the wave elevation $\sigma_{\zeta a}^2$ is calculated as

$$\sigma_{\zeta a}^2 = \sum_{j=1}^{N} S_{\zeta_a}(\omega_j)\Delta\omega \tag{23}$$

where $\sigma_{\zeta a}$ is the standard deviation of the wave elevation. Similarly, as the velocity amplitude of WEC corresponding to each wave component can be obtained

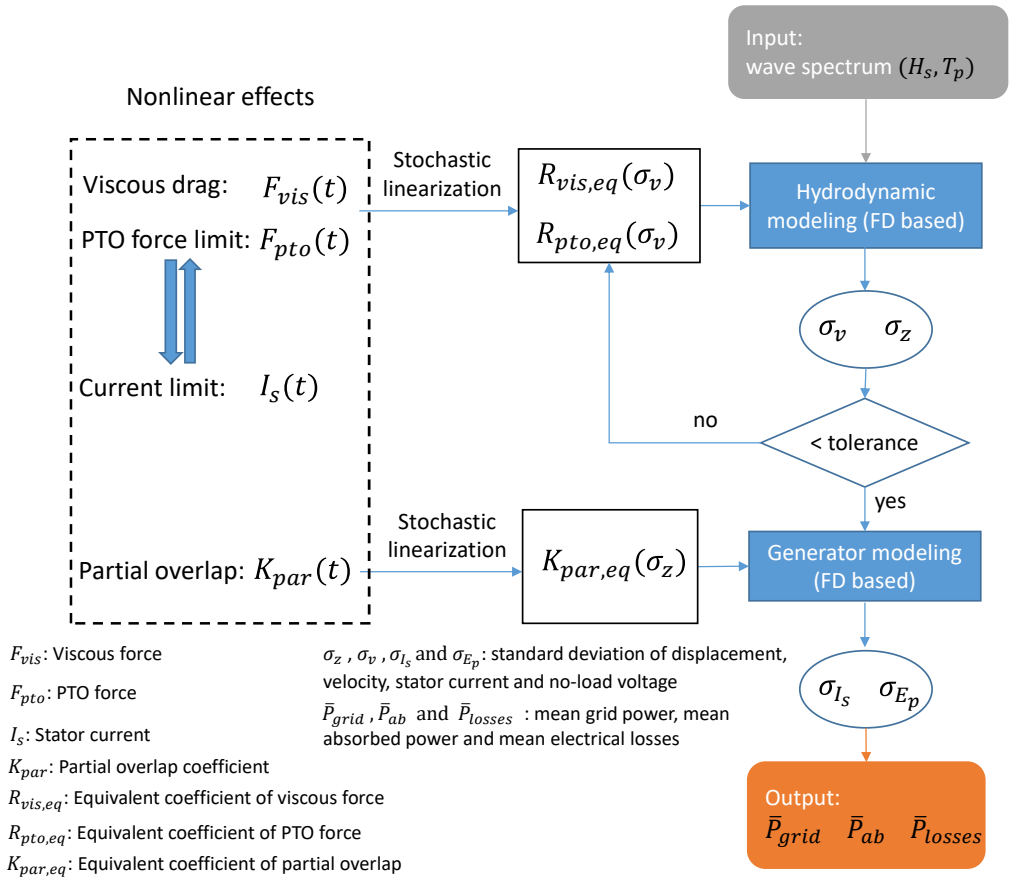

Fig. 2: Diagram of the proposed SD wave-to-wire modeling.

by (21), the standard deviation and spectral density of the WEC response can be calculated. Then, the mean absorbed power can be derived as

$$\begin{aligned}\overline{P}_{ab} &= \sum_{j=1}^{N} \frac{1}{2} R_{pto,eq} \, |\hat{v}(\omega_j)|^2 \\ &= \sum_{j=1}^{N} R_{pto,eq} S_v(\omega_j) \Delta\omega \\ &= R_{pto,eq} \sigma_v^2\end{aligned} \tag{24}$$

where S_v and σ_v denote the spectral density and standard deviation of the velocity of the WEC.

2) Generator modeling: While the hydrodynamic model described earlier is capable of predicting the mechanical power absorbed by the buoy, it does not capture the conversion of absorbed power into delivered electrical power, which is influenced by the electrical responses of the system. However, by assuming random phase distribution of wave inputs to the WEC system, it is feasible to represent the generator responses within the framework of SD modeling. This allows for the inclusion of electrical aspects and facilitates the description of the generator's behavior in the SD context.

Based on (5), the complex amplitude of the no-load voltage in each frequency component is expressed as

$$\hat{E}_p(\omega) = \sqrt{2} N_m \hat{v}(\omega) p l_s N_s k_w |\hat{B}_{gm}| L_{sta} K_{par,eq} \tag{25}$$

where $K_{par,eq}$ is the equivalent linear coefficient of the time-dependent partial overlap coefficient K_{par}. The linearization will be detailed in the following text.

The power taken by the generator winding, namely P_{wd}, at each frequency component is calculated as

$$\begin{aligned}P_{wd}(\omega) &= \frac{1}{2} \mathrm{Re}\{\hat{F}_{pto}(\omega) \hat{u}^*(\omega)\} \\ &= \frac{1}{2} |\hat{F}_{pto}(\omega)| |\hat{v}(\omega)| \\ &= \frac{1}{2} R_{pto,eq} |\hat{v}(\omega)|^2\end{aligned} \tag{26}$$

Thus, the magnitude of the complex amplitude of the stator current at each frequency component can be calculated as

$$|\hat{I}_s(\omega)| = \frac{R_{pto,eq} |\hat{v}(\omega)|^2}{m |\hat{E}_p(\omega)|} \tag{27}$$

As the effect of the PTO force limit has been incorporated by the equivalent linear coefficient $R_{pto,eq}$, the current limit is therefore taking effect correspondingly. Then, the standard deviation of the stator current is derived as

$$\sigma_{I_s} = \sqrt{\frac{1}{2} \sum_{j=1}^{N} |I_s(\omega_j)|^2} \tag{28}$$

At this stage, the hydrodynamic and electrical responses of the system can be estimated in a statistical

form using the SD modeling approach described earlier. However, to gain a deeper understanding of the generator's performance, it is necessary to determine the electrical losses in a statistical form, consistent with the expressions used in the TD approach. Specifically, the copper losses of the generator can be calculated as follows:

$$\begin{aligned}\overline{P}_{copper} &=< mI_s^2 R_t > \\ &= mR_t\sigma_{I_s}^2\end{aligned} \tag{29}$$

Assuming that the variable I_s follows the Gaussian distribution, it gives

$$< |I_s| >= \sqrt{\frac{2}{\pi}}\sigma_{I_s} \tag{30}$$

This enables the prediction of the converter losses, expressed as

$$\begin{aligned}\overline{P}_{conv} = \frac{1}{31}P_{convm} + \frac{20}{31I_{sm}}P_{convm} < |I_s| > + \\ \frac{10}{31I_{sm}^2}P_{convm} < I_s^2 >\end{aligned} \tag{31}$$

The iron losses are calculated as

$$\overline{P}_{Fes} = P_{Fe0}\big[m_{Fest}\big(\frac{\hat{B}_{st}}{B_0}\big)^2 + m_{Fesy}\big(\frac{\hat{B}_{sy}}{B_0}\big)^2\big]\frac{< f_e >}{f_0}K_{par,eq} \tag{32}$$

where $< f_e >$ can be related to the standard deviation of the absolute value of the buoy velocity, and assuming the Gaussian assumption of the response gives

$$\begin{aligned}< f_e > &= \frac{2\pi}{2\tau_p} < |v| > \\ &= \frac{\pi}{\tau_p}\sqrt{\frac{2}{\pi}}\sigma_v\end{aligned} \tag{33}$$

Therefore, the mean grid power can be derived as

$$\overline{P}_{grid} = \overline{P}_{wd} - \overline{P}_{copper} - \overline{P}_{Fes} - \overline{P}_{conv} \tag{34}$$

3) Stochastic linearization: The procedure for implementing stochastic linearization of the relevant nonlinear effects in the hydrodynamic stage has been demonstrated in previous references [12], [13], [16]. Therefore, in this discussion, we will provide a brief overview of the derivation of equivalent linear coefficients specifically for the nonlinearities associated with the electrical responses.

In the hydrodynamic stage, the equivalent linear coefficients $R_{\text{pto,eq}}$ and $R_{\text{vis,eq}}$ are considered to represent the effects of PTO force saturation and viscous force, respectively. The principle behind linearization is to achieve a balance between the expected value of the dissipated power and the power dissipated by an equivalent linear term. According to [12], the equivalent coefficient of a generic nonlinear force F_{non} in the hydrodynamic modeling can be calculated as follows:

$$\begin{aligned}R_{eq} &=< \frac{\partial F_{non}(u)}{\partial u} > \\ &= \int_{-\infty}^{\infty}\frac{\partial F_{non}(u)}{\partial u}p(u)\mathrm{d}u\end{aligned} \tag{35}$$

where F_{non} embodies the concerned nonlinear force, and $p(u)$ is the probability density function of the response u. Assuming the Gaussian process of the response, the probability density function is expressed as

$$p(h) = \frac{1}{\sigma_u\sqrt{2\pi}}\exp(-\frac{u^2}{2\sigma_u^2}) \tag{36}$$

As mentioned earlier, one specific nonlinear effect in linear generators arises from the partial overlap between the stator and translator of the machine. The power dissipated by a load in an electrical circuit can be generally expressed as follows:

$$P_{dis}(t) = \big[\frac{I_s(t)}{K_{par}(t)}\big]^2 R_t \tag{37}$$

Given random inputs, its expected value can be calculated as

$$< P_{dis} >=< I_s^2 >< \frac{1}{K_{par}^2} > R_t \tag{38}$$

It can be deduced that K_{par} is non-negative, thus (38) can be rewritten as

$$< P_{dis} >= \sigma_{I_s}^2\frac{1}{< K_{par}^2 >}R_t \tag{39}$$

As K_{par} is an even function with regard to the variable z, the equivalent linear coefficient $K_{eq,par}$ can be derived as

$$\begin{aligned}K_{par,eq} &= \sqrt{< K_{par}^2 >} \\ &= \sqrt{2\int_0^{\infty}K_{par}^2(z)p(z)\mathrm{d}z}\end{aligned} \tag{40}$$

The probability density function $p(z)$ of the buoy displacement is described by (36), assuming a Gaussian distribution. Notably, the iteration process is not required to obtain $K_{par,eq}$ since it depends on the standard deviation of the buoy displacement z. This standard deviation can be directly derived from the hydrodynamic modeling and serves as an input to the generator modeling, eliminating the need for additional iterations. This approach simplifies the calculation of $K_{par,eq}$ and enhances computational efficiency.

In SD modeling, the linearized representations of the viscous force and PTO force, namely $R_{vis,eq}$ and $R_{pto,eq}$, can also be obtained based on the principle of stochastic linearization. The derivation and verification have been detailed in [12], [13].

IV. Model Verification

This section presents the simulation results obtained from the SD W2W model, which are compared to those generated by the TD W2W model for verification. The simulations cover a range of wave states with different peak periods (T_p) and significant wave heights (H_s). The standard deviation of the responses, including buoy velocity, stator current, and induced no-load voltage, is compared between the SD and TD models in Figure 3. The relative errors of the SD model compared to the TD model are also shown. The results indicate that the SD model agrees reasonably well with the TD model, with maximum relative errors of 9 % for stator current, 4 % for no-load voltage, and 1 % for buoy velocity. The increase in significant wave height leads to slightly larger relative errors, attributed to the nonlinear effects becoming more dominant. The power spectral density analysis in Figure 4 further confirms the reasonable prediction of the SD model in capturing the frequency components of the stator current and no-load voltage. These findings demonstrate the effectiveness and accuracy of the proposed SD wave-to-wire model in simulating the dynamic behavior and electrical responses of the system.

The W2W modeling approach offers the advantage of providing a comprehensive understanding of the power conversion efficiency throughout the entire system operation. In order to further validate the accuracy of the established SD W2W model, the electrical power delivered to the grid and the power conversion efficiencies are calculated and compared with the results obtained from the TD W2W model. The power conversion efficiency, defined as the ratio of the delivered electrical power to the grid and the absorbed mechanical power by the floater, is of particular interest. Figure 5 illustrates the comparison between the SD model and the TD model in terms of grid power and power conversion efficiency. It can be observed that the proposed SD model accurately predicts the power and efficiency of the WEC. Even when the significant wave height reaches 4 m, the relative error between the SD and TD models remains below 7 % for power conversion efficiency estimation. For operational significant wave heights typically below 2.5 m, the relative error is less than 2 %. These results demonstrate the reliability and precision of the proposed SD W2W model in accurately estimating power conversion efficiency, making it a valuable tool for analyzing and optimizing the performance of WECs.

V. The Application to the Adjustment of PTO Parameters

Conventional FD models can be used to estimate the absorbed power of the WEC. Comparatively, the privilege of the W2W modeling is to reveal the delivered electrical power instead of the absorbed mechanical power. Previous studies have exemplified that the PTO damping coefficient corresponding to maximum absorbed power is not necessarily aligned with the value optimal for delivered electrical power. However, due

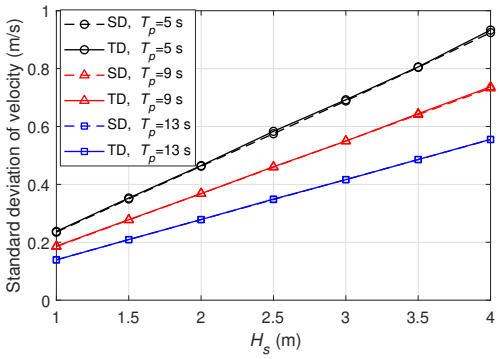

(a) Buoy velocity

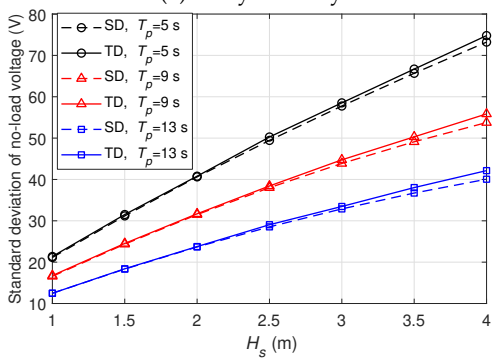

(b) No-load voltage

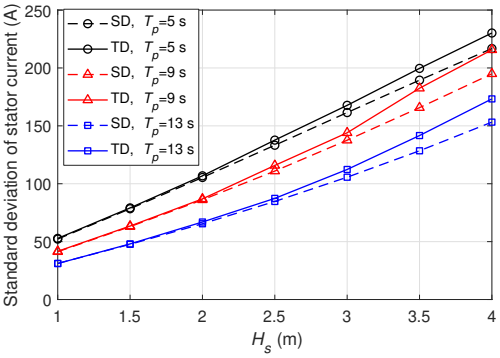

(c) Stator current

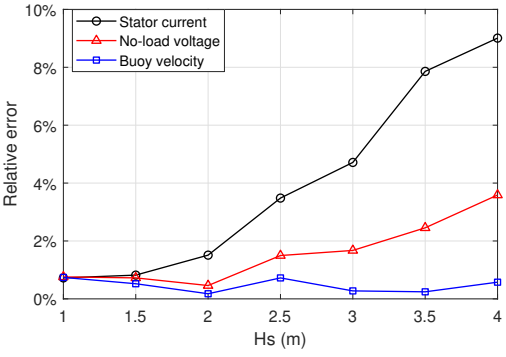

(d) The relative errors of the established SD model to the TD model averaged over the considered peak periods ($T_p = 5$ s, $T_p = 9$ s and $T_p = 13$ s).

Fig. 3: The standard deviation of the responses of the WEC in different wave states and the relative errors of the SD model to the TD model. ($B_{pto} = 60$ kNs/m)

to the high computational demand of TD W2W modeling, FD modeling is still predominately employed to determine the PTO parameters, especially in the early-stage evaluation of WECs. In the previous section, the reliability of the proposed SD W2W model has

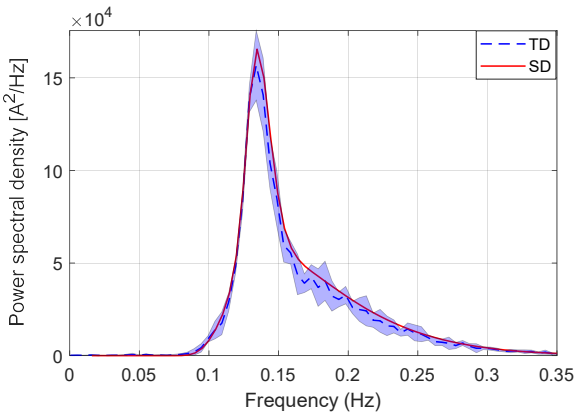

Fig. 4: The power spectral density of the stator current. ($B_{pto} = 60$ kNs/m, $H_s = 2.5$ m and $T_p = 7.5$ s) The shaded area represents the standard deviation of the results of the TD model.

been verified. In this section, the applicability of the proposed SD model to the tuning of PTO parameters is demonstrated. In this case study, the PTO damping is tuned by an exhaustive search scheme for various wave states. The search boundary is defined as 10 kNm/s to 250 kNs/m with a step of 5 kNs/m. SD, FD and TD models are used in the search scheme respectively. The set-up of the search scheme is identical for the three models.

In Figure 6, the PTO damping tuned by the FD modeling and SD W2W modeling is compared. As the FD modeling is fully linear, the selected PTO damping is consistent with the variation of the significant wave height. However, the SD modeling can reflect the effect of the significant wave height on the WEC performance, which indicates that the selected PTO damping increases with the significant wave height.

To investigate the influence of the PTO damping tuning on the power estimation, the electrical power of the WEC is calculated by the reference TD W2W modeling with the tuned PTO damping by the FD and SD models respectively. The results are shown in Figure 7. It can be seen that the power performance of the WEC is underestimated by using FD modeling to tune the PTO damping for maximum power production. The PTO damping tuned by the SD W2W model could better reflect the performance of the WEC. For instance, at the peak period of 10 s, the estimated electrical power with the PTO damping tuned by the SD model is 30 % higher than that with the PTO damping tuned by the FD modeling. In Figure 8, the three different models are used to reveal the relationship between the power and the PTO damping. It is visible that the SD model and TD model present highly comparable values for the maximum power, while the FD model corresponds to a much higher PTO damping. Besides, the SD model requires significantly less computational time to complete the PTO tuning process. As shown in Table II, the consumed time by the TD model for the case in Figure 8 is more than 20000 times longer than that by the SD model. It clearly suggests the competency of the proposed SD W2W model in the

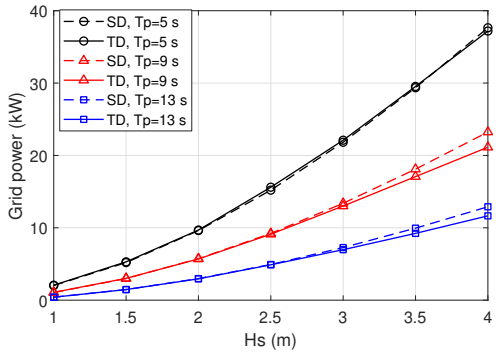

(a) Grid power

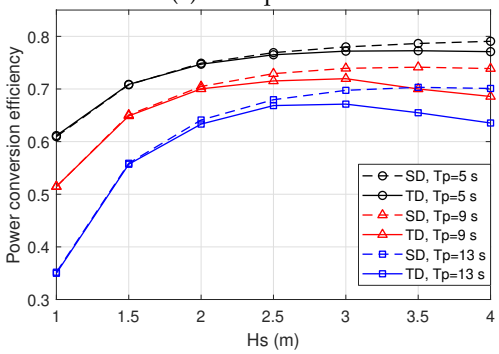

(b) Power conversion efficiency

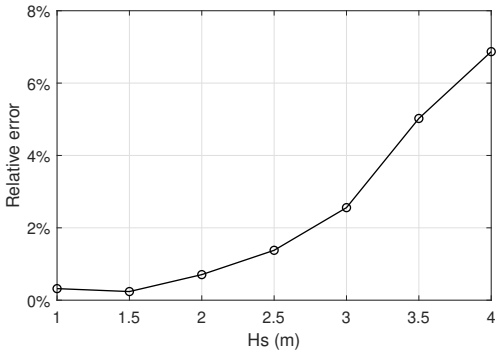

(c) The relative errors of the established SD model to the TD model with regard to the power conversion efficiency, and the values are averaged over the considered peak periods ($T_p = 5$ s, $T_p = 9$ s and $T_p = 13$ s).

Fig. 5: Grid power, copper losses and power conversion efficiency of the WEC in different wave states and the relative errors of the SD model to the TD model. ($B_{pto} = 60$ kNs/m)

application to the PTO tuning.

It is acknowledged that only the PTO damping adjustment is considered in this work, while the PTO stiffness is also an important parameter of the power production of the WEC. The proposed SD W2W model has the potential to be extended to cover the effects of the PTO stiffness although efforts are required to address the linearization of PTO force saturation with considering multiple variables. However, it is expected that incorporating the PTO stiffness would highly enlarge the applicability of the SD W2W model to more realistic cases.

Furthermore, it has to be noted that alternative approaches to SD modelling have also been proposed to cover the nonlinear force components typically repre-

TABLE II: The computational time of different models for the present case study.

Numerical modeling	FD	SD	TD
Computational time (s)	0.09	0.46	10800+

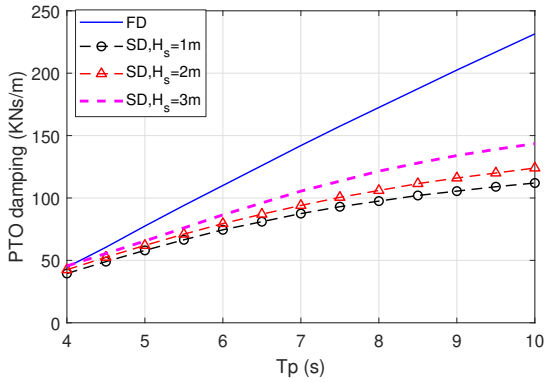

Fig. 6: The PTO damping selected based on the SD and FD models for maximizing the electrical power (SD) and absorbed power (FD).

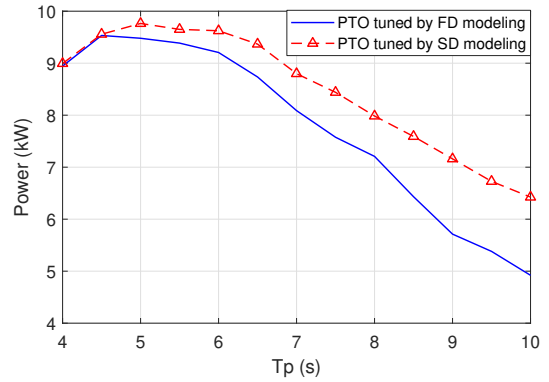

Fig. 7: The electrical power estimated by the TD W2W model with the PTO damping selected by the SD and FD models.

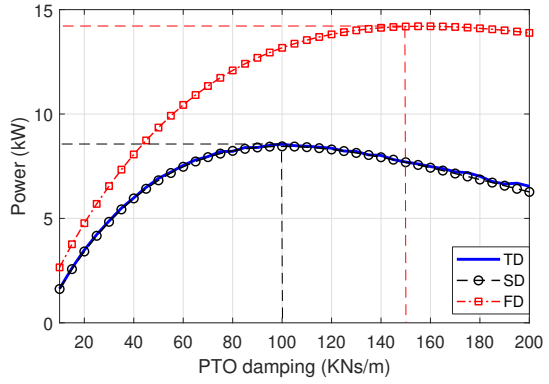

Fig. 8: The power estimate of WECs predicted by three different models with various values of the PTO damping. ($H_s = 2.0$ m and $T_p = 7.5$ s)

sented in TD models. For instance, the harmonic balance method was used in [30] to enable FD modelling to incorporate nonlinearities in WECs. The computational efficiency was significantly improved compared to TD modeling. However, to authors' knowledge, the applicability of harmonic balance method to the entire wave-to-wire process has not been verified.

VI. Conclusion

A SD W2W model is developed for a spherical point absorber with a linear PM generator. Stochastic linearization is implemented to incorporate typical nonlinear effects in both hydrodynamic and electrical stages of WECs. The proposed model is verified by a nonlinear TD W2W model, which suggests that the proposed model is associated with both adequate accuracy and high computational efficiency. The relative errors are not more than 4 % in operational conditions. Subsequently, the applicability of the SD model to adjusting PTO parameters is demonstrated. Compared with FD modeling, the PTO parameters selected based on the SD W2W model could better reveal the power performance of WECs. The high computational efficiency of the SD W2W model brings huge merit to the adjustment of PTO parameters where a large number of iterations are demanded.

References

[1] M. Penalba and J. V. Ringwood, "A review of wave-to-wire models for wave energy converters," *Energies*, vol. 9, no. 7, 2016.
[2] M. Folley, *Numerical Modelling of Wave Energy Converters*, 2016.
[3] M. Penalba and J. V. Ringwood, "A high-fidelity wave-to-wire model for wave energy converters," *Renewable energy*, vol. 134, pp. 367–378, 2019.
[4] M. Penalba, N. P. Sell, A. J. Hillis, and J. V. Ringwood, "Validating a wave-to-wire model for a wave energy converter—part i: The hydraulic transmission system," *Energies*, vol. 10, no. 7, p. 977, 2017.
[5] M. Penalba, J.-A. Cortajarena, and J. V. Ringwood, "Validating a wave-to-wire model for a wave energy converter—part ii: The electrical system," *Energies*, vol. 10, no. 7, p. 1002, 2017.
[6] J. Hals, J. Falnes, and T. Moan, "Constrained Optimal Control of a Heaving Buoy Wave-Energy Converter," *Journal of Offshore Mechanics and Arctic Engineering*, vol. 133, no. 1, p. 011401, 2010.
[7] J. Tan, H. Polinder, P. Wellens, and S. Miedema, "A feasibility study on downsizing of power take off system of wave energy converters," in *Developments in Renewable Energies Offshore*. CRC Press, 2020, pp. 140–148.
[8] D. Son and R. W. Yeung, "Real-time implementation and validation of optimal damping control for a permanent-magnet linear generator in wave energy extraction," *Applied Energy*, vol. 208, pp. 571–579, 2017.
[9] R. G. Coe and G. Bacelli, "Useful power maximization for wave energy converters," p. 529, 2023.
[10] J. Tan, X. Wang, H. Polinder, A. J. Laguna, and S. A. Miedema, "Downsizing the linear pm generator in wave energy conversion for improved economic feasibility," *Journal of Marine Science and Engineering*, vol. 10, no. 9, p. 1316, 2022.
[11] J. Tan, X. Wang, A. Jarquin Laguna, H. Polinder, and S. Miedema, "The influence of linear permanent magnet generator sizing on the techno-economic performance of a wave energy converter," in *2021 13th International Symposium on Linear Drives for Industry Applications (LDIA)*, 2021, pp. 1–6.
[12] M. Folley and T. Whittaker, "Spectral modelling of wave energy converters," *Coastal Engineering*, vol. 57, no. 10, pp. 892–897, 2010.
[13] J. Tan, H. Polinder, A. J. Laguna, and S. Miedema, "The application of the spectral domain modeling to the power take-off sizing of heaving wave energy converters," *Applied Ocean Research*, vol. 122, p. 103110, 2022.
[14] L. S. P. d. Silva, "Nonlinear stochastic analysis of wave energy converters via statistical linearization." Ph.D. dissertation, Universidade de São Paulo, 2019.

[15] L. S. da Silva, B. S. Cazzolato, N. Y. Sergiienko, B. Ding, H. M. Morishita, and C. P. Pesce, "Statistical linearization of the morison's equation applied to wave energy converters," *Journal of Ocean Engineering and Marine Energy*, vol. 6, no. 2, pp. 157–169, 2020.

[16] L. Silva, N. Sergiienko, C. Pesce, B. Ding, B. Cazzolato, and H. Morishita, "Stochastic analysis of nonlinear wave energy converters via statistical linearization," *Applied Ocean Research*, vol. 95, p. 102023, 2020.

[17] P. D. Spanos, F. M. Strati, G. Malara, and F. Arena, "An approach for non-linear stochastic analysis of u-shaped owc wave energy converters," *Probabilistic Engineering Mechanics*, vol. 54, pp. 44–52, 2018.

[18] S. Gunawardane, M. Folley, and S. Sanjaya, "Spectral-domain modelling of the non-linear hydrostatic stiffness of a heaving-sphere wave energy converter," in *Proceedings of the 28th International Symposium on Transport Phenomena, Peradeniya, Sri Lanka*, 2017, pp. 22–24.

[19] G. Giorgi, M. Penalba, and J. Ringwood, "Nonlinear hydrodynamic models for heaving buoy wave energy converters," 2016.

[20] H. Polinder, M. E. C. Damen, and F. Gardner, "Linear PM generator system for wave energy conversion in the AWS," *IEEE Transactions on Energy Conversion*, vol. 19, no. 3, pp. 583–589, 2004.

[21] P. Tokat, *Performance evaluation and life cycle cost analysis of the electrical generation unit of a wave energy converter*. Chalmers Tekniska Hogskola (Sweden), 2018.

[22] M. Prado and H. Polinder, *Case study of the Archimedes Wave Swing (AWS) direct drive wave energy pilot plant*. Woodhead Publishing Limited, 2013. [Online]. Available: http://dx.doi.org/10.1533/9780857097491.2.195

[23] Johannes Falnes, *Ocean waves and Oscillating systems*, 2003.

[24] J. M. J. Journée, W. W. Massie, and R. H. M. Huijsmans, *Offshore hydrodynamics*, 2015.

[25] W. Cummins, W. Iiuhl, and A. Uinm, "The impulse response function and ship motions," 1962.

[26] T. Pérez and T. Fossen, "Time-vs. frequency-domain identification of parametric radiation force models for marine structures at zero speed," *Modeling, Identification and Control*, vol. 29, no. 1, pp. 1–19, 2008.

[27] G. Giorgi and J. V. Ringwood, "Consistency of viscous drag identification tests for wave energy applications," *12th European Wave and Tidal Energy Conference*, pp. 1–8, 2017.

[28] H. Polinder, F. van der Pijl, G.-J. de Vilder, and P. Tavner, "Comparison of direct-drive and geared generator concepts for wind turbines," *IEEE Transactions on Energy Conversion*, vol. 21, no. 3, pp. 725–733, 2006.

[29] M. Folley and T. Whittaker, "Validating a spectral-domain model of an owc using physical model data," *International Journal of Marine Energy*, vol. 2, pp. 1–11, 2013.

[30] A. Mérigaud and J. V. Ringwood, "A nonlinear frequency-domain approach for numerical simulation of wave energy converters," *IEEE Transactions on Sustainable Energy*, vol. 9, no. 1, pp. 86–94, 2017.